1970–1986 *Nucleic Acids Research, 2014, Vol. 42, No. 3* *Published online 11 November 2013*
doi:10.1093/nar/gkt1118

The Drosophila RNA-binding protein HOW controls the stability of *dgrasp* mRNA in the follicular epithelium

Giuliano Giuliani[1], Fabrizio Giuliani[1], Talila Volk[2] and Catherine Rabouille[1,3,*]

[1]Hubrecht Institute-KNAW & University Medical Center Utrecht, Uppsalalaan 8, 3584 CT Utrecht, The Netherlands, [2]Department of Molecular Genetics, Weizmann Institute of Science, Rehovot 76100, Israel and [3]The Department of Cell Biology, UMC Utrecht, The Netherlands

Received April 9, 2013; Revised October 18, 2013; Accepted October 22, 2013

ABSTRACT

Post-transcriptional regulation of RNA stability and localization underlies a wide array of developmental processes, such as axon guidance and epithelial morphogenesis. In *Drosophila*, ectopic expression of the classically Golgi peripheral protein dGRASP at the plasma membrane is achieved through its mRNA targeting at key developmental time-points, in a process critical to follicular epithelium integrity. However, the *trans*-acting factors that tightly regulate the spatio-temporal dynamics of *dgrasp* are unknown. Using an *in silico* approach, we identified two putative HOW Response Elements (HRE1 and HRE2) within the *dgrasp* open reading frame for binding to Held Out Wings (HOW), a member of the Signal Transduction and Activation of RNA family of RNA-binding proteins. Using RNA immunoprecipitations, we confirmed this by showing that the short cytoplasmic isoform of HOW binds directly to *dgrasp* HRE1. Furthermore, HOW loss of function *in vivo* leads to a significant decrease in *dgrasp* mRNA levels. We demonstrate that HRE1 protects *dgrasp* mRNA from cytoplasmic degradation, but does not mediate its targeting. We propose that this binding event promotes the formation of ribonucleoprotein particles that ensure *dgrasp* stability during transport to the basal plasma membrane, thus enabling the local translation of *dgrasp* for its roles at non-Golgi locations.

INTRODUCTION

Tissue and cell physiology is governed by gene expression that consists of a large spectrum of processes that allow for the versatility and adaptability of an organism. Gene expression is regulated at multiple levels. One mode of regulation is at the post-transcriptional level, where mRNA levels are fine-tuned by appropriate degradation or stabilization. The latter is critical for localized mRNAs that need to be translationally repressed but stabilized until they reach their target site. RNA-binding proteins (RBPs) are known to regulate the overall stability of mRNA as they can either recruit RNA degradation machinery or protect RNA from degradation (1–3).

Traditionally *Drosophila melanogaster* represents a strong model for elucidating post-transcriptional regulation events (4–6). Studies of the *Drosophila* egg-chambers, aiming to understand gene regulation by RNA metabolism (such as localization, stability and translation) have led to the characterization of a large number of key factors implicated in these processes (7–9), as well as shed light to their importance for correct development, specification and homeostasis of this tissue (10–12). The integrity of the follicular epithelium covering the *Drosophila* oocyte is also thought to depend upon a number of transcripts that, at specific stages of development, become localized in the proximity of the baso-lateral plasma membrane of the follicle cells, in a region that we name the 'open zone of contact' (open ZOC) (13,14). One of these transcripts is *dgrasp* that encodes a protein known to be associated peripherally to the Golgi membrane, with many roles in the Golgi architecture and dynamics (15). Recently, this protein has also been shown to mediate two types of unconventional secretion (16). This includes the Golgi bypass of alpha PS1 integrin subunit (αPS1) at stage 10B of *Drosophila* oogenesis, during which it is transported to the open ZOC in a manner that deviates from the classical pathway (ER > Golgi > PM) (13).

One of the striking features of *dgrasp* mRNA in the follicular epithelium is the tight window of expression. Beginning at stage 10A of oogenesis, *dgrasp* mRNA appears as cytoplasmic foci that we interpret to be

*To whom correspondence should be addressed. Tel: +31 30 2121941; Fax: +31 30 2516464; Email: c.rabouille@hubrecht.eu

ribonucleoprotein particles (RNPs) that are then targeted to the open ZOC at stage 10B (14). There, *dgrasp* mRNA appears to be locally translated (13). To understand the post-transcriptional regulation and dynamics of *dgrasp* mRNA, we aimed to identify RBPs involved in its metabolism.

The Signal Transduction and Activation of RNA (STAR) family is one of the most evolutionarily conserved groups of RBPs across the animal kingdom and controls a wide range of developmental events by regulating alternative splicing and translational repression of specific mRNA targets. In mammals, for instance, the most-studied member of the STAR family, Sam68, has an active role during spermatogenesis where it modulates alternative splicing in male germ cells (17). Its evolutionarily related counterpart Quaking (QKI) regulates myelination by Schwann cells and oligodendrocytes by controlling the splicing of myelin-associated glycoprotein (MAG) and other myelin targets (18–20). Interestingly, QKI also regulates muscle fibre maturation in zebrafish by stabilizing *Gli2a* transcripts (21). In *Caenorhabditis elegans*, the STAR protein GLD-1 is a translational repressor and promotes germ cell differentiation (22,23) and ASD-2 is required for alternative splicing (24).

The *Drosophila* member of the STAR family Held Out Wings (HOW), like its mammalian orthologue QKI, is highly expressed in muscles, tendons (25–28) and glial cells (29,30), where it plays an essential role in controlling the mRNA levels of an array of target genes during development (31). HOW exerts various functions on its target RNAs: it facilitates the alternative splicing of *stripe A*, a transcription factor essential for tendon cell maturation and mediates specific splicing of the transcript encoding for the septate junction protein Neurexin IV, thereby controlling glial cell maturation. It also functions by reducing mRNA levels of various targets. For example, during gastrulation, HOW-dependent down-regulation of *cdc25/string*, which encodes for a cell cycle promoting phosphatase, is essential to inhibit cell division in invaginating mesodermal cell (32).

The hallmark of STAR proteins is the presence of a single extended maxi-KH RNA-binding domain. Structurally, HOW, like two other STAR proteins QKI and ASD2, contains a single maxi-KH RNA-binding motif that is flanked by two additional conserved N- and C-terminal sequences, named the QUA1 and QUA2 domains, respectively (28).

Interestingly, the *HOW* gene has three alternative splice variants, which are named according to their length, HOW(Long), HOW(Medium) and HOW(Short). The expression of HOW(L) begins at early embryonic stages, while HOW(S) is expressed in later stages of differentiated tissues. HOW(M) was recently predicted by Flybase and its expression remains to be characterized. HOW(S) and HOW(L) are almost identical in their amino acid sequence, except that HOW(S) lacks the HPYQR signal peptide essential for nuclear retention. Consequently, HOW(S) predominantly localizes to the cytoplasm whereas HOW(L) is mostly found in the nucleus (33,34).

Here, we perform a computer-based comparative analysis to identify putative RBPs that interact with and regulate *dgrasp* mRNA. We propose that *dgrasp* is a novel target of HOW(S) and that this interaction is critical for *dgrasp* mRNA stabilization.

MATERIALS AND METHODS

In silico prediction of putative RBP-binding sites

RNA-Binding Protein DataBase (RBPDB) developed by (35) is a web-free database of RNA-binding experiments (http://rbpdb.ccbr.utoronto.ca/) that provides a scanning tool to identify RBP-binding sites in the given query sequences. It contains binding data on 272 RBPs, including 71 that have motifs in position weight matrix format (PWM) and 36 sets of sequences of *in vivo*-bound transcripts from immunoprecipitation experiments.

Briefly, the strategy pursued for the RBP prediction consists in independently running orthologous sequences of the RNA of interest through RBPDB to identify sites matching the known RBP-binding sites annotated in the database. Only putative sites with relative scores greater than the set threshold of 70% were included. RBPDB outputs for each RNA sequence were then exported in an excel file for comparison. This was followed by manual curation that removed RBPs sites not conserved in all the species included in the analysis.

For the *Pitx2* 3′UTRs *in silico* analysis, the orthologous sequences of five vertebrate species (human, mouse, chicken, zebrafish and xenopus) were considered. For *dgrasp*, we used the open reading frame (ORF) and the 3′UTR of orthologous sequences of six *Drosophila* species (*D. melanogaster, D. simulans, D. sechellia, D. ananassae, D. erecta* and *D. yakuba*). For *Neurexin IV*, sequences of a portion of intron 3 of 11 different *Drosophila* species (*D. melanogaster, D. simulans, D. sechellia, D. ananassae, D. erecta*, *D. yakuba, D. pseudobscura, D. persimilis, D. willistoni, D. mojavensis, D. virilis*) were used. The genomic intervals of intron 3 used as inputs for analysis are: *D. melanogaster* 5163–5232 nt; *D. simulans* 5111–5180 nt; *D. sechellia* 5120–5189 nt; *D. erecta* 5058–5127 nt; *D. ananassae* 4599–4662 nt; *D. yakuba* 5145–5214 nt; *D. pseudobscura* 4985–5055 nt; *D. persimilis* 4966–5031 nt; *D. virilis* 923–996 nt; *D. mojavensis* 5467–5542 nt; *D. grimshawi* 5399–5470 nt. Sequence interval numbering is with respect to the translational start site (ATG).

RNA structure prediction with RNApromo

For prediction of RNA structures, we used the 'Segal tool' RNApromo (http://genie.weizmann.ac.il/pubs/rnamotifs08/rnamotifs08_predict.html). This tool predicts a structural motif common to a set of given RNA sequences. The folding algorithm used in the Segal method is the 'Vienna package' and the default parameters that we used for the prediction are the following: Number of motifs to predict, 3; Stem size flexibility, 3; Loop size flexibility, 1; Background distribution, Binomia-short motifs.

Specifically, the prediction of *dgrasp* HRE1 and HRE2 structures was performed using sequences from six

Drosophila species (*D. melanogaster, D. simulans, D. sechellia, D. erecta, D. ananassae and D. yakuba*). For the prediction of HRE1, the RNA intervals entered into RNApromo structure are: *D. melanogaster* 862–894 nt; *D. simulans* 876–909 nt; *D. sechellia* 877–909 nt; *D. erecta* 871–903 nt; *D. ananassae* 874–906 nt *and D. yakuba* 871–903 nt. For the prediction of HRE2, the RNA interval used are: *D. melanogaster* 989–1030 nt; *D. simulans* 1004–1045 nt; *D. sechellia* 1004–1045 nt; *D. erecta* 993–1033 nt; *D. ananassae* 1068–1107 nt *and D. yakuba* 992–1033 nt. Note that sequence interval coordinates are with respect to the translational start site (ATG).

We also use the Vienna RNAalifold WebServer (http://rna.tbi.univie.ac.at/) to predict the secondary structures of HRE1 and HRE2 motifs. For the prediction of each HRE motif using this method, a multiple sequence alignment of the six *Drosophila* sequences was obtained with ClustalW2 (with the same genetic intervals as for the RNApromo analysis) and used as input in the RNAalifold WebServer. Default settings of the web pipetline RNAalifold were used. As for the RNApromo analysis, the prediction of HRE1 and HRE2 structures was performed using sequences from six *Drosophila* species (*D. melanogaster, D. simulans, D. sechellia, D. erecta, D. ananassae and D. yakuba*). For the prediction of HRE1 and HRE2 structures, the same RNA sequence intervals used in RNApromo were entered.

Fly strains

Drosophila melanogaster stocks were raised on standard cornmeal-yeast agar medium at 25°C unless otherwise stated. *OregonR* line was used as the wild-type reference strain and is referred to as WT. The other lines used (coming from the Bloomington stock centre http://flystocks.bio.indiana.edu/) unless otherwise stated) are: w^{1118}; $HOW^{stru\text{-}3R\text{-}3}$, *FRT82B/TM6B, Tb; hs::Gal4/Gla, Bc, Elp; c355::Gal4; pr pwn hs::flp/CyO; +/Ki ry; UAS-HOW(S)-3HA* and *UAS-HOW(L)-3HA* (unpublished data, Talila Volk), *w; FRT82B ubi::GFP/TM3, Sb*. The additional *Drosophila* species *D. simulans*, *D. sechellia, D. erecta, D. yakuba, D. ananassae* were obtained from the Ehime-fly [the *Drosophila* stocks of Ehime University, Japan (http://kyotofly.kit.jp/cgi-bin/ehime/index.cgi)].

For overexpression experiments of HOW(S)-3HA and HOW(L)-3HA fusion proteins in ovaries, 2-day-old *hs::Gal4/+; UAS-HOW(S)-3HA/+* and *hs::Gal4/+; UAS- HOW(L)-3HA/+* female progeny fattened on yeast [obtained from the cross between *w; UAS-HOW(S)-3HA* or *w; UAS-HOW(L)-3HA* and *hs::Gal4/Gla, Bc, Elp*, respectively] were incubated for 2 h at 37°C, and then let to recover for five additional hours at 25°C prior to dissection.

$HOW^{stru\text{-}3R\text{-}3}$ homozygous mutant clones in the follicular epithelium were generated using the heat shock-inducible Flp-FRT system (36). Female progeny *hs::FLP/+;* $HOW^{stru\text{-}3R\text{-}3}$, *FRT82B/FRT82B ubi::GFP* obtained from the cross of males *hs::FLP/+;* $HOW^{stru\text{-}3R\text{-}3}$, *FRT82B/Ki, ry* to females *hs::flip/+; FRT82B ubi::GFP/Ki, ry* were collected upon eclosion and raised for 2 days in presence of yeast at 22°C. During this time, flies were exposed to two heat-shock treatments (one per day) at 37°C for 1 h prior to dissection for ovaries collection.

RNA isolation and reverse transcription

Total RNA was extracted from ovaries at different stages of development with TRIzol® Reagent (Invitrogen) in accordance with the protocol of the manufacturer. The isolated RNA was treated with RNase-free DNase I (Sigma) to eliminate possible genomic DNA contamination. RNA was reverse transcribed into cDNA with GoScript™ Reverse Transcription System (Promega) and random primers (Promega) according to manufacturer.

Immunolabelling

Ovary staining was performed as described previously in (13). Briefly, ovaries from 2-day-old virgin flies were dissected, fixed for 15 min in 4% PFA and finally permeabilized in 0.1% TritonX. Permeabilized ovaries were incubated with primary antibodies overnight at 4°C; FITC- and TRITC-conjugated secondary antibodies (Invitrogen) incubations were done for 3 h at room temperature. The following antibodies were used: rabbit anti-HOW antibody (1:300), mouse anti-α-spectrin 3A9 antibody (1:20, DSHB) and mouse anti-HA antibody 16B12 (1:50, Covance). TRITC-conjugated phalloidin (1:200, Sigma) was used for visualization of the plasma membrane in egg-chambers overexpressing HOW(S)-HA and HOW(L)-HA transgenes. Egg chambers were incubated with far-red fluorescent TO-PRO®-3 (1:500; Life Technologies) for 30 min for nuclear staining. Samples were mounted in ProLong Gold anti-fade reagent (Invitrogen) on glass slides and imaged with Leica SPE Confocal Microscope.

Fluorescent *in situ* hybridization

After fixation as described above, following dissection and fixation in 4% PFA, ovaries were stored in 100% methanol. Full-length *dgrasp* and *gfp* sense and antisense digoxigenin-labelled RNA probes were synthesized using DIG RNA Labelling Kit (Roche) according to the manufacturer. Fluorescent *in situ* hybridization (FISH) was performed as described in (13). Briefly, fixed ovaries were hybridized with a digoxigenin-labelled RNA probe overnight at 55°C. After washing, signal was developed by using an anti-digoxigenin-POD antibody (1:100, Roche) and the TSA (Tyramide Signal Amplification) Cyanine 3 System (PerkinElmer). Following tyramide reaction, samples were incubated for 1h with mouse anti-α-spectrin 3A9 antibody (1:20, DSHB) to outline the plasma membrane.

Fluorescence quantification with ImageJ

The measurement of the fluorescence intensity of *dgrasp* FISH in $HOW^{-/-}$ and $HOW^{+/-}$ cells was performed using images captured at identical confocal settings. Stacks of

images were taken and the four slices showing the brightest labelling were used for the measurements of average pixel intensities. This was done in Image J using the line measurement tool to draw the boundaries of the $HOW^{-/-}$ clones. Background was estimated from a laser-off image and was subtracted. Average pixel intensities was also measured outside the clones in the surrounding areas of identical sizes ($HOW^{+/-}$ cells). Mean intensities for $HOW^{-/-}$ and $HOW^{+/-}$ were averaged and then statistically compared using an unpaired two-tailed Student's *t*-test ($n = 20$).

RNA–protein co-immunoprecipitation

Ovaries from 40 females [WT or overexpressing HA-tagged HOW(L) and HOW(S)] were dissected and homogenized in RNA immunoprecipitation (RIP) lysis buffer.

Each lysate was divided into two samples; one was used for immunoprecipitation with either rabbit anti-HOW (5 µg) (37) or mouse anti-HA 16B12 (5 µg) (Covance) antibodies, and the second was used with control rabbit or mouse IgG (5 µg). The immunoprecipitation was performed using the Magna RIP™ RNA-Binding Protein Immunoprecipitation kit (Millipore) as described by the manufacturer. The IP samples and the input (10% of the lysates) were phenol–chloroform precipitated to extract the RNA. An amount of 20 ng of RNA from each fraction (input, HOW or HA IP and IgG IP fractions) was subjected to a reverse transcription (RT) reaction using random primers to generate cDNA libraries. Equivalent amounts of cDNA were then used for quantitative PCR reactions to detect the enrichment of *dgrasp*, *Neurexin IV* and *shotgun* mRNAs in the different immunoprecipitation.

Real-time RT–qPCR and quantitation

Real-time RT–PCR (RT-qPCR) for quantification of mRNA amount was performed as described by (38) with an MyIQ Real-time PCR systems (Bio-rad) and with iQ™ SYBR® Green Supermix (Bio-rad) used for detecting the fluorescence of amplified products. Real-time reaction was carried out as follows: pre-denaturing at 95°C for 3 min, followed by 45 cycles at 95°C for 30 s and 60°C for 1 min. Melting curves were generated for the final PCR products by decreasing the temperature to 65°C for 15 s followed by an increase in temperature to 95°C. Fluorescence was measured at 0.2°C increments. Real-time PCR MyIQ software (Bio-rad) was used to determine the amplification cycle in which product accumulation was above the threshold cycle values (C_T). Real-time PCR C_T values were analysed using the $2^{-\Delta CT}$ method (39).

In RIP experiments, the measured amount of *dgrasp*, *Neurexin IV* and *shotgun* mRNAs in each immunoprecipitation (IP) are presented as the relative enrichment in either HOW or HA RIP compared with IgG RIP [$C_{T[dgrasp(\text{HOW or HA IP})]} - C_{T[dgrasp(\text{IgG IP})]}$]. The different x-fold inductions of *dgrasp*, *Neurexin IV* and *shotgun* transcripts in the HOW and HA immunoprecipitations were also calculated by the $2^{-\Delta CT}$ method (39).

The primer sequences used for RT–qPCR reactions are the following:

	Forward	Reverse
dgrasp	5′-CACCGAAGGCTACCAC GTA-3′	5′-TTGTCAACGTTCTGGCG GAG-3′
shotgun	5′-GACGTTTGCACCTTCAA CGT-3′	5′-CCGCAGAATCTCGTATT CGA-3′
Neurexin IV	5′-CTCGGATGGACGCGTG ATTA-3′	5′-GTTGAAGAGTCGGGAG GAGC-3′

For the quantification of *dgrasp* mRNA levels in single egg chambers of control and $HOW^{-/-}$ mutant ovaries, the housekeeping gene *gpdh* was analysed as internal standard. ΔC_T-values were calculated as follows: $C_{T(gpdh)} - C_{T(dgrasp)}$, and were normalized to *gpdh* levels. The *dgrasp* mRNA fold change in egg chambers carrying $HOW^{-/-}$ mutant clones was calculated by the $2^{-\Delta CT}$ method (39), with values normalized to *gpdh* and relative to control ovaries.

	Forward	Reverse
dgrasp	5′-CACCGAAGGCTACCAC GTA-3′	5′-TTGTCAACGTTCTGGCG GAG-3′
gpdh	5′-AAATCGCGGAGCCAAG TAGT-3′	5′-CACGATTTTCGCTATGG CCG-3′

In the RNA degradation assay, upon quantification by RT–qPCR, the values obtained for each target gene (*dgrasp-FL* and *dgrasp-ΔHRE1*) were normalized against values of the endogenous housekeeping human gene *GAPDH* (from the Caco-2 cell extract, see below) using the $2^{-\Delta CT}$ method (39). Results of each condition were plotted as the percentage of synthetic *dgrasp-FL* and *dgrasp-ΔHRE1* RNAs remaining as a function of time from the starting point T0. Sequences of primers used for the RT–qPCR are shown below.

Caco-2 cell extract preparation

Approximately 10^8 Caco-2 cells were washed two times with 40 ml ice-cold wash buffer (150 mM sucrose, 33 mM ammonium chloride, 7 mM potassium chloride, 4.5 mM magnesium acetate, 30 mM HEPES, pH 7.4). Cells were then resuspended in 1 ml standard reaction as described in (40) and were disrupted via passages through a thin syringe needle. After spinning for 10 min at 10 000 rpm at 4°C, the supernatant is collected and stored on ice waiting to start the *in vitro* mRNA degradation assay. The lysate can be stored in small aliquot at −80°C.

In vitro mRNA degradation assay

The *in vitro* degradation assay was adapted from (41). pCS2+ full-length *dgrasp* (*dgrasp-FL*) and ΔHRE1 mutant (*dgrasp-ΔHRE1*) templates were linearized with *ApaI*. *dgrasp* RNAs (*dgrasp-FL* and *dgrasp-ΔHRE1*) were synthesized using mMESSAGE mMACHINE® High Yield Capped RNA Transcription Kits (Ambion).

Prior to initiate RNA degradation reactions, 5 µl of 1 µg/µl *in vitro* translated HOW(S)-HA were pre-incubated with 5 µg of *in vitro* transcribed *dgrasp* mRNA at room temperature for 10 min in binding buffer [100 mM

KCl, 5 mM MgCl, 10 mM HEPES, pH 7.0, 0.5% NonidetP-40, 1 mM DTT, 100 U/ml Rnasin RNase inhibitor (Promega), 2 mM vanadyl ribonucleoside complex solution and 25 µl/ml protease inhibitor cocktail] in a final volume of 40 µl. This was followed by the addition of 90 µg of Caco-2 cell extracts (for preparation of Caco-2 cell extract see section above) in presence or absence of 100 U/ml of the general RNase inhibitors (RNasin®) (Promega).

Incubations containing synthetic RNAs, HOW(S)-HA and Caco-2 cell extracts were carried at 30°C for 0, 45 and 180 min. The RNA was purified by adding one volume of TRIzol (Invitrogen) and two volumes of chloroform, and precipitated from ethanol as described by (42). cDNA libraries for each reaction were made using 500 ng of total RNA following the protocol described above, and *in vitro* decay of full-length WT and ΔHRE1 mutant *dgrasp* RNAs was assessed by RT–qPCR reactions using the following primer set

	Forward	Reserve
dgrasp FL	5′-CACCGAAGGCTACCAC GTA-3′	5′-TTGTCAACGTTCTGGCG GAG-3′
GAPDH	5′-TGCACCACCAACTGCTT AGC-3′	5′-GGCATGGACTGTGGTC ATGAG-3′

Levels of both *dgrasp-FL* and *dgrasp-ΔHRE1* RNAs were normalized to those of endogenous human *GAPDH* mRNA (coming from the Caco-2 lysate) and plotted as the percentage of synthetic *dgrasp-FL* and *dgrasp-ΔHRE1* RNAs remaining as a function of time from T0 as explained above.

In vitro interaction assay

Full-length *dgrasp* RNA (FL) and *dgrasp* fragments (NT, CT2, CT2-ΔHRE1, CT2-ΔHRE2 and CT2-ΔHRE1-2) as well as *Neurexin IV* intron 3 were prepared by *in vitro* transcription using as templates PCR products carrying the T7 promoter on the forward primers using the MEGAscript® T7 Kit, (Ambion®).

PCR products were obtained using specific sets of primers (below). *In vitro* transcribed RNAs were purified with a phenol-chloroform step and precipitated in isopropanol prior to elution in nuclease-free dH_2O.

	Forward	Reverse
dgrasp FL	5′-TTAATACGACTCACTAT AGGGAGAAGCCACAGC ATCCAT-3′	5′-CTCGAGGCGTTTCCAG CCTGATTCAC
NT	5′-TTAATACGACTCACTAT AGGGAGAAGCCACAGC ATCCAT-3′	5′-CTCGAGGCGGGAATGC GATGCAAATAGCC-3′
CT2	5′-TAATACGACTCACTATA GGGGACCACCGACTAT TGAGCCAC-3′	5′-CTGTGGTGCAGAGAAC ATGG-3′
Intron 3	5′-TAATACGACTCACTATA GGGGTGA	5′-TCGAAGACGTTGTAAT GGATAGAG-3′
Neurexin IV	CACTGCGACTAACTAGAT TGG-3′	

CT2-ΔHRE1, CT2-ΔHRE2 and CT2-ΔHRE1-2 fragments were generated by site-directed mutagenesis using mutagenic primers (below) and CT2 primer pair (CT2F and CT2R) as flanking primers.

	Forward	Reverse
HRE1mut	5′-GAGGCTACCGATGCCT TTTTCGCTGCGCTCGAA TCGC-3′	5′-GCGATTCGAGCGCAGC GAAAAAGGCATCGGTA GCCTC-3′
HRE2mut	5′-CCATTGCCGCCACCAGT TTTTATCTTTATACCC-3′	5′-GGGTATAAAGATAAAA ACTGGTGGCGGCAATG G-3′

HOW(S)-HA was cloned into the pcDNA3.1 vector and translated *in vitro* using TNTR-Coupled Reticulocyte Lysate System following manufacturer instructions (Promega). Binding assays were performed by adding 5 µl (~5 µg) of the translation mixture to 1 µg of *in vitro* transcribed RNA for 30 min at RT in 250 µl of binding buffer [100 mM KCl, 5 mM MgCl, 10 mM HEPES, pH 7.0, 0.5% NonidetP-40, 1 mM DTT, 100 U/ml Rnasin RNase inhibitor (Promega), 2 mM vanadyl ribonucleoside complex solution and 25 µl/ml protease inhibitor cocktail].

ProteinG magnetic beads (Invitrogen) were first washed with binding buffer [lacking glycerol and tRNA, and containing 0.5% BSA (Sigma)], and incubated with mouse anti-HA 16B12 (Covance) antibody at a concentration of 5 µg/50 µl of beads at RT for 30 min. Upon washing to remove unbound anti-HA antibody, 50 µl of the resuspended beads was added to each binding reaction overnight at 4°C.

RNA was phenol–chloroform precipitated from samples. Input RNA was used as positive control. cDNA was prepared with random primers, followed by RT–PCR with the primer combination used above for the generation of *dgrasp* FL, NT, CT2 and *Neurexin IV intron 3*.

Generation of pUAST-*CT dgrasp*::GFP and pUAST-*CT2 dgrasp*::GFP transgenic lines

GFP-tagged *CT-* and *CT2-dgrasp* fragments were generated by PCR reaction using the following primers

	Forward	Reverse
CT2-dgrasp	5′-ATGGTACCAACATGCCAC CGACTATTGAGCCAC-3′	5′-ATGCGGCCGCTGTGGT GCAGAGAACATGG-3′
CT-dgrasp	5′-ATGGTACCAACATGATTG GCTTCGGCTATTTGC-3′	5′-ATGCGGCCGCTTTCCA GCCTGATTCACTG-3′

First, they were cloned into pRMeGFP vector using *KpnI* and *NotI* restriction sites, upstream of the GFP sequence. GFP-tagged *CT-* and *CT2-dgrasp* fragments were then sub-cloned into the pUAST vector (43) using *KpnI* and *XbaI* sites. Finally, *Drosophila* stable transgenic lines were generated with Bestgene (Chino Hills, CA, USA). Several independent lines were obtained for both constructs. Insertions on the third chromosome were used for all the experiments, and expression was driven by the follicular epithelium specific driver *c355::Gal4* driver. 2-day-old *c355::Gal4/+; +/+; UAS-CTdgrasp::GFP/+* and *c355::Gal4/+; +/+; UAS-CT2::dgrasp::GFP/+*

female progeny fattened on yeast at 25°C were dissected to collect ovaries.

RESULTS

Comparative *in silico* analysis predicts HOW response elements in *dgrasp* mRNA

In order to identify potential RBPs regulating *dgrasp* mRNA, we performed a comparative genomics-based orthologous RNA analysis using the online RBPDB (35). This strategy consists of running homologous mRNA sequences in multiple species against this database. The predicted outcome of putative RBP signatures found in one transcript is then compared with the others, and only the RBP motifs shared by all homologues are taken into consideration for further analysis (see 'Materials and Methods' section for further details).

To validate the sensitivity/robustness of this approach, we first ran transcripts for which RBPs have been experimentally characterized. MBNL1 interacts with the 3′UTR of the *Pitx2* transcript (44). Analysis of the 3′UTR sequences of the *Pitx2* transcripts from different species (human, mouse, dog, zebrafish, *xenopus*) using our strategy (Supplementary Figure S1A) predicts signatures for 17 putative RBPs (Supplementary Figure S1B). Notably, the all MBNL1 sites, experimentally characterized by (44), were efficiently predicted by our method (Supplementary Figure S1C), therefore validating the reliability of our approach.

Next, to identify potential RBPs regulating *dgrasp* mRNA, we set out to analyse the *dgrasp* mRNA sequences (consisting of the ORFs and 3′UTRs, but not 5′UTRs) from six different *Drosophila* species for which we could confidently predict the boundary of the 3′UTR: *D. melanogaster, D. simulans, D. sechellia, D. ananassae, D. erecta* and *D. yakuba*. First, we verified that *dgrasp* mRNA of these species showed a comparable spatio-temporal expression to *D. melanogaster,* i.e. with a similar initial up-regulation and formation of RNPs in the cytoplasm of the follicle cells at stage 10A followed by targeting of the *dgrasp* transcripts near the open ZOC at stage 10B (Supplementary Figure S2).

We then performed our *in silico* approach that led to the prediction of putative signatures for binding to 18 RBPs (Figure 1A). Two of these signatures are conserved putative binding elements for the STAR family member QKI/GLD-1/HOW (called HOW Response Elements, HRE, Figure 1B and C) and RNA secondary structure softwares (RNApromo and RNAalifold) predict that these sites are present on loops (Figure 1B and Supplementary Figure S3).

Our decision to focus on HOW relates to the fact that homozygous mutant escapers of the weak *HOW* allele, HOW^{r17} exhibit blisters in the wings (25), a phenotype that resembles the wing phenotype reported in the $dgrasp^{100.2}$ homozygous mutant escapers (13). In the absence of a reported *HOW* follicular epithelial mutant phenotype, the wing phenotype suggested a possible genetic interaction between these two genes, making HOW a strong candidate for post-transcriptional regulation of *dgrasp* mRNA.

To validate the reliability of the predicted *dgrasp* HREs, we used the same approach with sequences of a known HOW target, *Neurexin IV* (29). A number of HREs have been identified within *Neurexin IV* intron 3 in the proximity of the splice acceptance boundary and the interaction of HOW in this region is crucial for the generation of different Neurexin IV protein isoforms (34). Our analysis successfully led to the identification of these same HREs in the intron 3 of *Neurexin IV* gene (Supplementary Figure S4).

Furthermore, we used a matrix predicting binding motif for the *C. elegans* HOW orthologue GLD-1. GLD-1 has recently been shown to associate with hundreds of germline mRNAs, and these mRNAs all exhibit motifs predicted to bind GLD-1 (7 mers ± 1 or 2 variations). These data were used to build a *C. elegans* matrix [for description of the matrix see (45)]. Strikingly, using this same matrix, the identification of the two putative HREs in the *dgrasp* RNA ORF were also predicted (personal communication). Interestingly, endogenous *C. elegans grasp* mRNA (Y42H9AR.1) was pulled down by GLD-1 immunoprecipitation [see (45), their Supplementary Figure S1] and also displays two GLD-1 response elements in the C-terminus of the ORF (at sites 907–913 nt and 987–993 nt with respect to the TSS). Taken together, these results make HOW a strong candidate regulator of *dgrasp* mRNA metabolism.

HOW binds *dgrasp* transcript *in vivo*

To test whether HOW binds to *dgrasp* mRNA *in vivo* in the follicular epithelium, we performed RIP assays using ovaries dissected from young WT *D. melanogaster*. Endogenous HOW in complex with its mRNA targets was immunoprecipitated using an anti-HOW antibody. *Neurexin IV* mRNA was used as a positive control since it is expressed in the follicular epithelium (13) as well as being a well-established target of HOW, while *shotgun* mRNA, the *Drosophila* DE-cadherin homologue, that has not been reported to be a HOW target was chosen as a negative control. As expected, RT–PCR from IgG RIP (negative control) did not yield amplification of *Neurexin IV*, *dgrasp* or *shotgun* mRNA (Figure 2A). Conversely, both *Neurexin IV* and *dgrasp* transcripts were detected in the cDNA library of the HOW RIP, whereas *shotgun* mRNA was not (Figure 2A). To confirm these results, we performed real-time RT–qPCR of the same RIPs. *dgrasp* and *Neurexin IV* mRNAs are significantly enriched (13.5- and 60-fold, respectively) in the HOW RIP when compared with IgG, whereas *shotgun* mRNA did not show any significant enrichment (Figure 2B). In summary, these results suggest that endogenous HOW binds endogenous *dgrasp* mRNA in the fly ovaries.

HOW(S) is enriched at the open ZOC

To investigate further whether HOW regulates *dgrasp* mRNA in the follicular epithelium, we examined the expression and localization of the endogenous HOW protein

A

List of Shared RNA-binding proteins

RBP name	site in d.mel *dgrasp* mRNA	RBP name	site in d.mel *dgrasp* mRNA	RBP name	site in d.mel *dgrasp mRNA*
RBFOX1-3/a2bp1 (1)	1523 (UGCAUG)	MBNL1/mbl (10)	161 (UGCU)	RBM4/lark (2)	520 (CGCG)
ACO1/irp-1A & B (3)	617 (CAGAGC)		284 (UGCU)		948 (CGUG)
	1202 (CAGUGC)		307 (UGCU)	SFRS13A/SC35 (5)	66 (ACAGGAC)
	1361 (CAGUGA)		420 (UGCC)		315 (CGAGGGC)
EIF4B/eIF-4B (4)	69 (GGAC)		479 (CGCU)		327 (CGAGAGC)
	1409 (GGAC)		1083 (UGCC)		837 (CAAGACC)
	1424 (CCUGGAC)		1175 (CGCU)		1657 (AAAGGCA)
	1654 (GGAA)		1205 (UGCC)	SFRS9/SF2 (3)	68 (AGGAC)
ELAVL1/elav (4)	493 (GUUU)		1268 UGCC		470 (AGCAG)
	1436 (GUUA)		1402 (UGCU)		473 (AGCAG)
	1468 (GUUU)	NONO/nonA (1)	560 (AGGGA)	SNRPA/snf (2)	326 (ACGAGAG)
	1603 (AUUU)	QKI/HOW (2)	872 (CCCUAACCGC)		1542 (AUUGCAU)
KHDRBS3/qkr54B (5)	1418 (GCUAAA)		1008 (AGCCAACAUC)	Vts1 (5)	91 (GCCGGAC)
	1553 (AAUAAU)	RBMX/tra2 (10)	28 (CCCG)		285 (GCUGGGC)
	1566 (AUUAAU)		51 (CCAC)		379 (GCAGGAC)
	1578 (AAUAAA)		218 (CCAG)		691 (GCCGGAG)
	1586 (AAUAAA)		248 (CCCU)		894 (GCAGGCC)
FUS/caz (1)	1221 (GGUG)		1006 (CCAC)	YBX1/yps (4)	285 (GCUGGG)
SFRS1/SF2 (4)	98 (UGGA)		1117 (CCAG)		305 (UCUGCU)
	503 (UGGA)		1186 (CCAG)		548 (CCUGGG)
	561 (GGGA)		1297 (CCAC)		1171 (GCUGCG)
	1426 (UGGA)		1300 (CCAG)	YTHDC1/yt521-b (2)	296 (GCAUAC)
			1518 (CCAU)		1301 (CAGUAC)

B

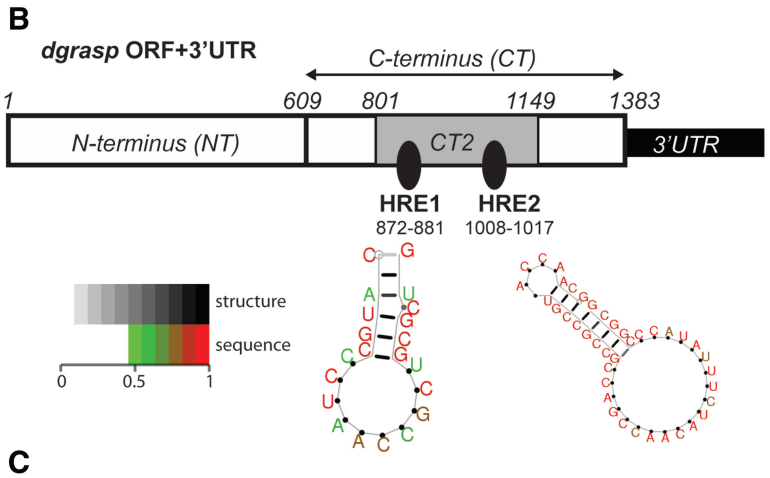

C

HRE1 motif

```
d.mel   834 TTCAAGACCTACTTCAATCCGGATGAGGCTACCGATGCCCTAACCGCTGCGCTCGAATCG 894
d.sim   849 TTCAAGACCTACTTCAATCCGGATGAGGCTACCGATGCCCTAACCGCTGCGCTCGAATCG 909
d.sec   849 TTCAAGACCTACTTCAATCCGGATGAGGCTACCGATGCCCTAACCGCTGCGCTCGAATCG 909
d.yak   843 TTCAAGACCTACTTCAATCCGGATGAGGCTACCGATGCACTAACTGCGGCGTTGGAAACG 903
d.ere   843 TTCAAGACCTACTTTAATCCGGATGAGGCTACCGATGCACTTACTGCGGCGCTGGAAACG 903
d.ana   846 TTCAAGACCTACTTTAATCCTGATGATGCTACAGATGCTCTCACTGCAGCGCTGGAGACT 906
            ************** ***** ***** *****.***** ** ** ** *** * **.:*
```

HRE2 motif

```
d.mel   993 CCATTGCCGCCACCAGCCAACATCTTTATACCCGGCGTTTTCGATCCCAGTACGCAGCAA 1053
d.sim  1008 CCAATGCCGCCGCCAGCCAACATCTTCATACCCGGCGTTTTTGATCCCAGTACGCAGCAA 1068
d.sec  1008 CCAATGCCGCCGCCAGCCAACATCTTTATACCCGGCGTTTTCGATCCCAGTACGCAGCAA 1068
d.yak   996 CCATTGCCGCCACCAGCCAACATCTTTATACCCGGCGTTTTTGATCCCAGTGCGCAACAA 1056
d.ere   996 CCATTGCCGCCCCCAGCTAACATCTTTATACCCGGCGTTTTTGATCCCAGTACGCAGCAA 1056
d.ana  1071 CCATTGCCGCCGCCAGCCAACATTTTTATTCCCGGGGTCTATGATCCCAGCACAAAACAG 1131
            ***:******* ***** ***** ** **:***** ** *: ******** .*..*.**.
```

Figure 1. Computational prediction of HREs in *dgrasp* mRNA ORF. (**A**) Outcome of the 18 predicted RBPs from the comparative RBPDB *in silico* analysis using *dgrasp* mRNA sequence (ORF and 3′UTR) from *D. melanogaster*, *D. simulans*, *D. sechellia*, *D. ananassae*, *D. erecta* and *D. yakuba*. The vertebrate RBPs are listed in blue whereas the *D. melanogaster* homologues are in green. The numbers of predicted sites for each RBP, with respect to the translational start site (ATG), are shown in red. (**B**) Cartoon representation of the two HOW Response Elements (HREs) predicted at the C-terminus of the ORF of *D. melanogaster dgrasp* at position 872–881 nt (HRE1) and 1008–1017 nt (HRE2) with respect to the translational start site (ATG). The structure prediction of the two HREs using the RNA secondary structure program

(continued)

by immunofluorescence. HOW is expressed in this tissue from stage 8, and is both nuclear (arrows) and cytoplasmic (Figure 3A). The nuclear localization corresponds to HOW(L) that exhibits a nuclear localization signal (NLS) in its sequence (27), whereas the cytoplasmic pool is likely to correspond to HOW(S) (46,47). In addition, at stage 10, a pool of HOW is enriched near the baso-lateral plasma membrane, including the open ZOC (Figure 3A), in a similar location to that of *dgrasp* mRNA at this specific stage (Figure 3B).

To identify the HOW isoform that localizes near the plasma membrane at stage 10 of *Drosophila* oogenesis, both HA-tagged isoforms were independently expressed in the follicular epithelium using the UAS-GAL4 system (48). As predicted, HOW(L)-HA localized to the nucleus of the follicle cells at all stages (Figure 3C), whereas HOW(S)-HA was present in the cytoplasm as well as near the open ZOC at stage 10 (Figure 3D). This suggests that HOW(S), but not HOW(L), binds to *dgrasp* mRNA.

dgrasp mRNA is a direct target of HOW(S)

To test whether *dgrasp* is a target for HOW(S), we performed RIP on extracts from ovaries overexpressing HOW(S)-HA and HOW(L)-HA using an anti-HA antibody. *dgrasp* mRNA was detected in the cDNA library generated from the HOW(S)-HA IP, but not from the HOW(L)-HA or IgG IPs. Conversely, *Neurexin IV* mRNA was detected only from the cDNA library of the HOW(L)-HA, but not HOW(S)-HA (Figure 2C), showing the specificity of the approach. We confirmed these results by real-time RT–qPCR that shows a 62.3-fold enrichment of *dgrasp* mRNA in the HOW(S)-HA IP when compared with HOW(L), whereas *Neurexin IV* transcripts were 85.7-fold more enriched in HOW(L)-HA IP than in the HOW(S) (Figure 2D). Taken together, our results show that HOW(S) forms a complex with endogenous *dgrasp* mRNA.

As HOW(S) contains a conserved KH RNA-binding domain, it was predicted to bind *dgrasp* directly. To test this, *in vitro* translated HOW(S)-HA was incubated in presence of *in vitro* transcribed full-length *dgrasp* RNA (Figure 4A). The protein was immunoprecipitated using an anti-HA antibody followed by RT–PCR to detect bound *dgrasp*. As expected, IgG RIP did not lead to *dgrasp* mRNA amplification, whereas HA RIP showed that, indeed, HOW(S) binds *dgrasp* transcript directly (Figure 4B).

Next, we asked whether the HREs that we identified (Figure 1B) were required for HOW(S) binding to *dgrasp* mRNA. To test this, we carried out *in vitro* synthesis of two *dgrasp* mRNA fragments, one encompassing the region where the two HREs were located (CT2), and the second corresponding to the N-terminus (NT) that did not contain any HREs (Figure 1B). Using the same approach as described in the previous paragraph, we showed that HOW(S)-HA specifically bound CT2 but not NT (Figure 4C), indicating that the HREs are likely to play a functional role in binding.

To confirm this finding and to assess which of the two predicted HREs are required for HOW(S) binding, CT2 fragment mutant isoforms, where either or both of the predicted HREs replaced by a string of Us (CT2-ΔHRE1, CT2-ΔHRE2 and CT2-ΔHRE1−2) were synthesized *in vitro* as above.

Using two independent RNA structure prediction programs [RNApromo (Segal lab) and RNAalifold (Vienna)], we first checked that this substitution does not disrupt the loop structure in which the HREs are located (Supplementary Figure S3C). We then tested the interaction of these fragments with purified HOW(S)-HA. As predicted, HOW(S)-HA did not interact with CT2-ΔHRE1-2, but still interacted with CT2-ΔHRE2 (Figure 4D), suggesting that only one of the HREs (HRE1, CCTAAC, 872–881nt, Figure 1B) is functional and recognized by HOW(S) for binding.

Loss of HOW expression affects *dgrasp* mRNA stability

To investigate the function of HOW binding to *dgrasp* mRNA in the follicular epithelium, we induced homozygous mutant clones carrying the strong loss of function allele $HOW^{stru\text{-}3R\text{-}3}$ in this tissue (49) (see 'Materials and Methods' section).

In control ovaries (siblings of the same background but not expressing the flippase) as well as in the heterozygous tissue surrounding the $HOW^{stru\text{-}3R\text{-}3}$ mutant clones, the expression of *dgrasp* and its localization is comparable to WT and with clear targeting to the open ZOC (Figure 5A and B) as well as cytoplasmic foci corresponding to RNPs (arrowheads in Figure 5B, insert) (13). In $HOW^{stru\text{-}3R\text{-}3}$ mutant clones, however, the levels of *dgrasp* mRNA are reduced ~7-fold when compared with the neighbouring heterozygote cells (Figure 5B, C). We confirmed this reduction by real-time RT–qPCR on single stage 10 egg chambers. In those in which *HOW* mutant clones were induced, *dgrasp* levels were reduced by 21% when compared with control egg chambers (Figure 5D; $n = 6$).

The loss of *dgrasp* mRNA in $HOW^{stru\text{-}3R\text{-}3}$ clones suggests that HOW is required for *dgrasp* mRNA stability, either for the formation of RNPs protecting the RNA against degradation, or for its targeting to the open ZOC. Close examination of the $HOW^{stru\text{-}3R\text{-}3}$ clones showed that *dgrasp* RNPs were completely absent in the $HOW^{stru\text{-}3R\text{-}3}$ clones and that when a faint *dgrasp* mRNA pool was observed, it was targeted to the plasma membrane (arrows in Figure 5B, insert). This suggests

Figure 1. Continued
RNA promo (Segal lab http://genie.weizmann.ac.il/pubs/rnamotifs08/rnamotifs08_predict.html) is presented. The two HRE sites are marked by arrows and are predicted to be in loops. Sequence positions in the predicted structure are colour-coded according to their probability (>0.5 by default) with scale ranging from green (low probability = 0.5) to red (high probability = 1). (**C**) Alignment of the coding regions of the *dgrasp* drosophilid orthologues. The two predicted HRE sequences are coloured in red. *dgrasp* coding sequences of *D. melanogaster*, *D. simulans*, *D. sechellia*, *D. ananassae*, *D. erecta* and *D. yakuba* were used for the ClustalW2-based alignment.

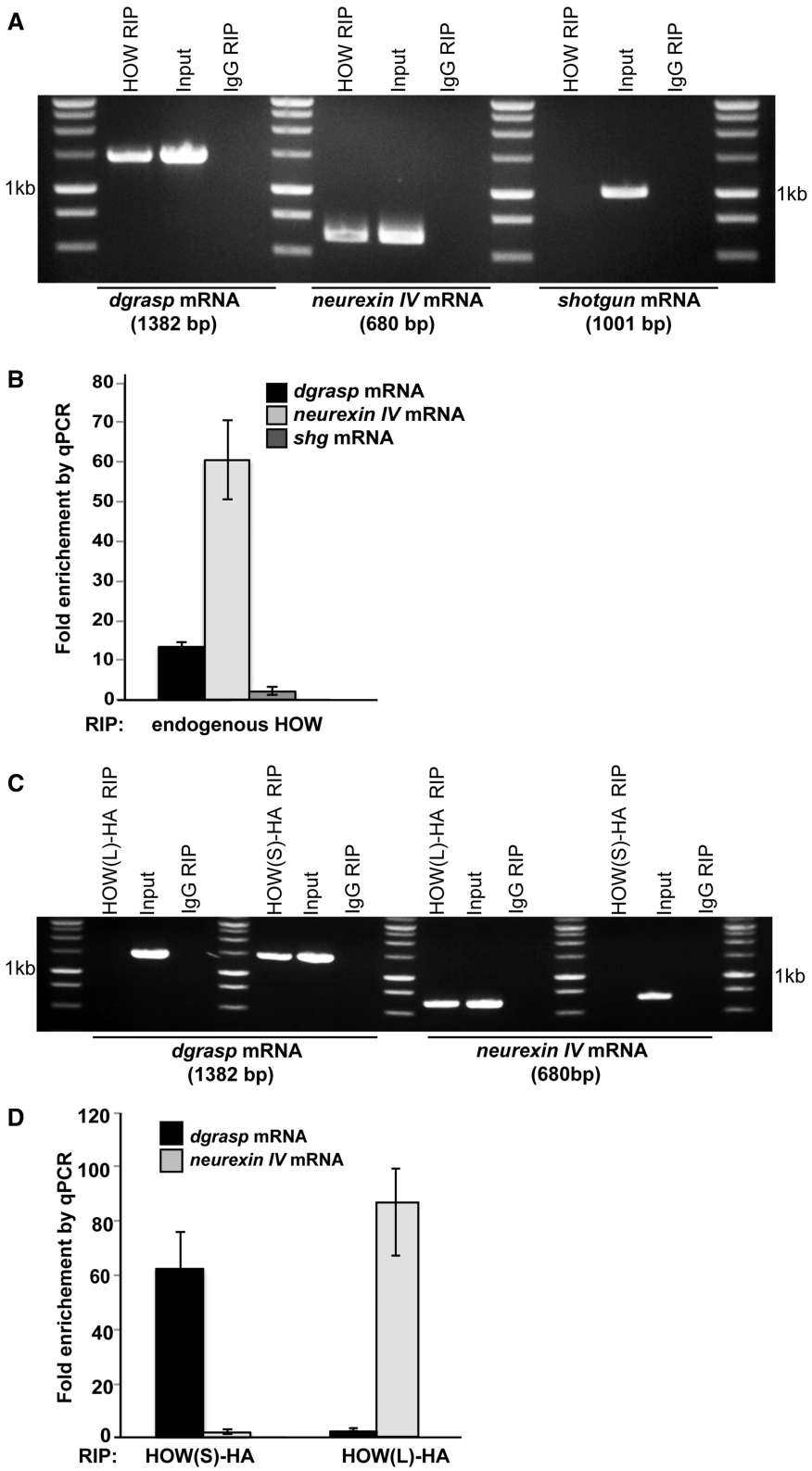

Figure 2. Endogenous HOW binds *dgrasp* mRNA in *Drosophila* ovaries. (**A**) Agarose gel electrophoresis of RT-PCR reactions from RIP from WT *Drosophila* ovaries using anti-HOW (HOW RIP) or IgG (IgG RIP). Transcripts scored in the RIP reactions are *dgrasp* and *Neurexin IV* mRNAs; *shotgun* was used as a negative control. (**B**) Relative enrichment of endogenous *dgrasp, Neurexin IV* and *shotgun* in HOW RIP compared with IgG RIP measured by real-time RT–qPCR. Values are means ± standard deviations (SD) (error bars) ($n = 3$). (**C**) Agarose electrophoresis of PCR product from endogenous *dgrasp* and *Neurexin IV* mRNA immunoprecipitated from *Drosophila* ovaries overexpressing HOW(S)-HA and HOW(L)-HA using an anti-HA antibody [HOW(L)-HA RIP and HOW(S)-HA RIP] or an IgG as control (IgG RIP). Note that *dgrasp* mRNA binds HOW(S)-HA. (**D**) Relative enrichment of *dgrasp* and *Neurexin IV* in HOW(S)-HA and HOW(L)-HA RIP when compared with IgG RIP measured by real-time RT–qPCR. Values are means ± SD (error bars) ($n = 3$).

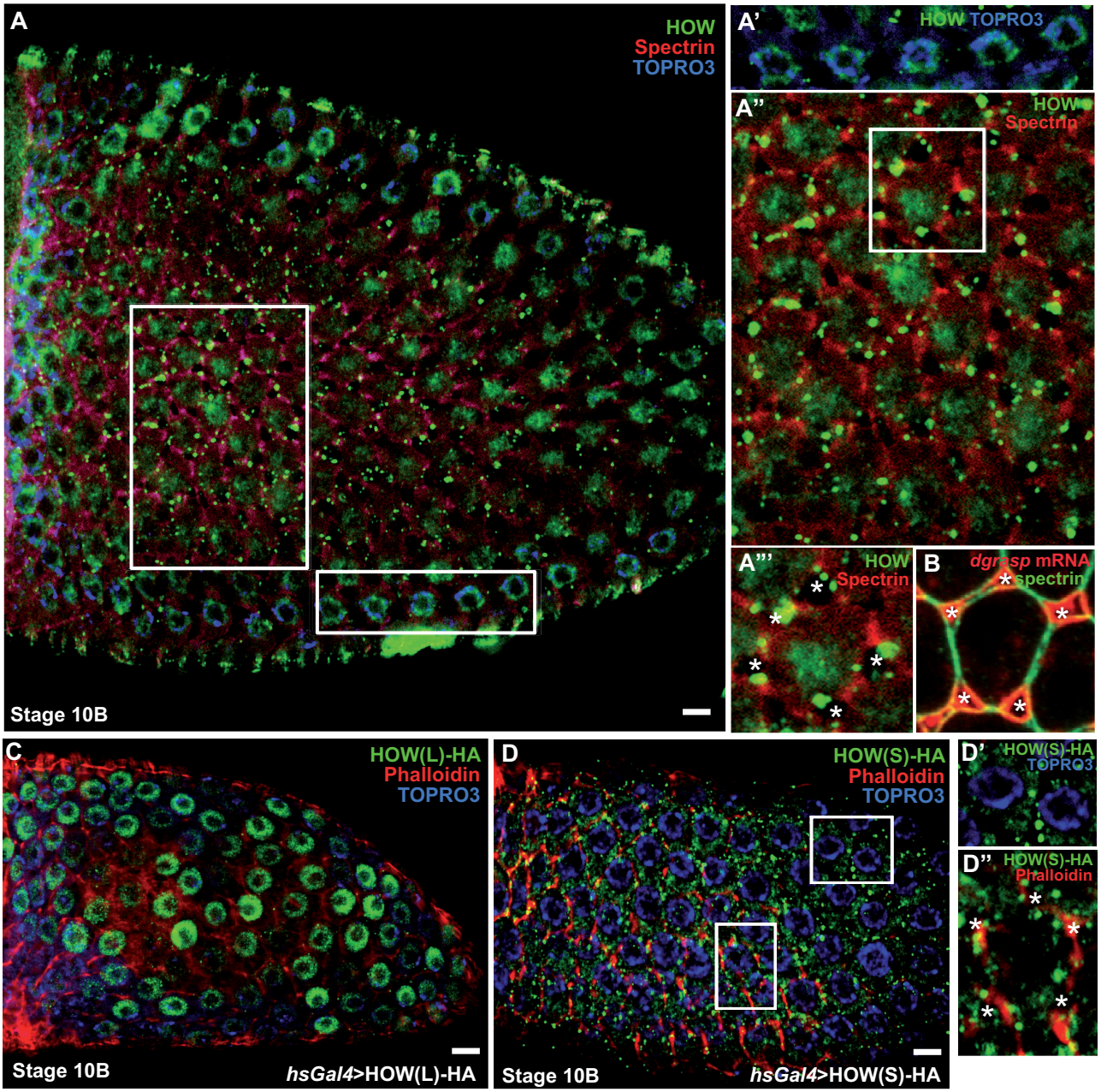

Figure 3. HOW(S) localizes near the basal plasma membrane of follicle cells at stage 10 of oogenesis. **A–A‴.** Immunolocalization of endogenous HOW using an anti-HOW antibody (green) in stage 10 *Drosophila* follicular epithelium. α-spectrin marks the cell cortex (red) and TOPRO3 marks the nucleus (blue). HOW is localized in the nucleus (see top insert, A′) as well as in the cytoplasm (A″), in particular in dots around the open ZOC (asterisks in insert bottom, A‴) at the basal side of the follicle cells. Note that the nucleolus (unstained dot in the middle of the nucleus is very large). (**B**) FISH localization of *dgrasp* mRNA (red) with respect to the open ZOC (asterisks). α-spectrin (green) marks the cell cortex. (**C**) Immunolocalization of HOW(L)-HA overexpressed in the follicular epithelium using the UAS-Gal4 system under the control of a heat-shock promoter. Anti-HA labelling (green) shows that HOW(L) is restricted to the nucleus at all stages in the follicular epithelium development. Phalloidin (red) stains the actin of the cell cortex and TO-PRO®-3 (blue) marks the nucleus. (**D–D″**) Immunolocalization of HOW(S)-HA (using an anti-HA antibody, green) overexpressed in the follicular epithelium using the UAS-Gal4 system under the control of a heat shock promoter, Phalloidin (red) stains the actin of the cell cortex and TO-PRO®-3 (blue) marks the nucleus. Inserts show that HOW(S) is absent from the nucleus (D′) whereas it is enriched around the open ZOC (asterisks, bottom insert). Scale bars: 10 μm.

that HOW might be required for RNP formation leading, in turn, to *dgrasp* stabilization.

To test this hypothesis, we designed an *in vitro* degradation assay to compare the stability of full-length *in vitro* transcribed *dgrasp* RNA with that of a form of *dgrasp* where HRE1 was mutated (*dgrasp*-ΔHRE1). These two RNAs were incubated with HOW(S)-HA and successively exposed to Caco-2 cell lysate extract as a source of RNases for an increasing length of time (0, 45 and 180 min), both in the presence and absence of RNase inhibitors. Real-time RT–qPCR was used to measure the amount of RNA left in each sample.

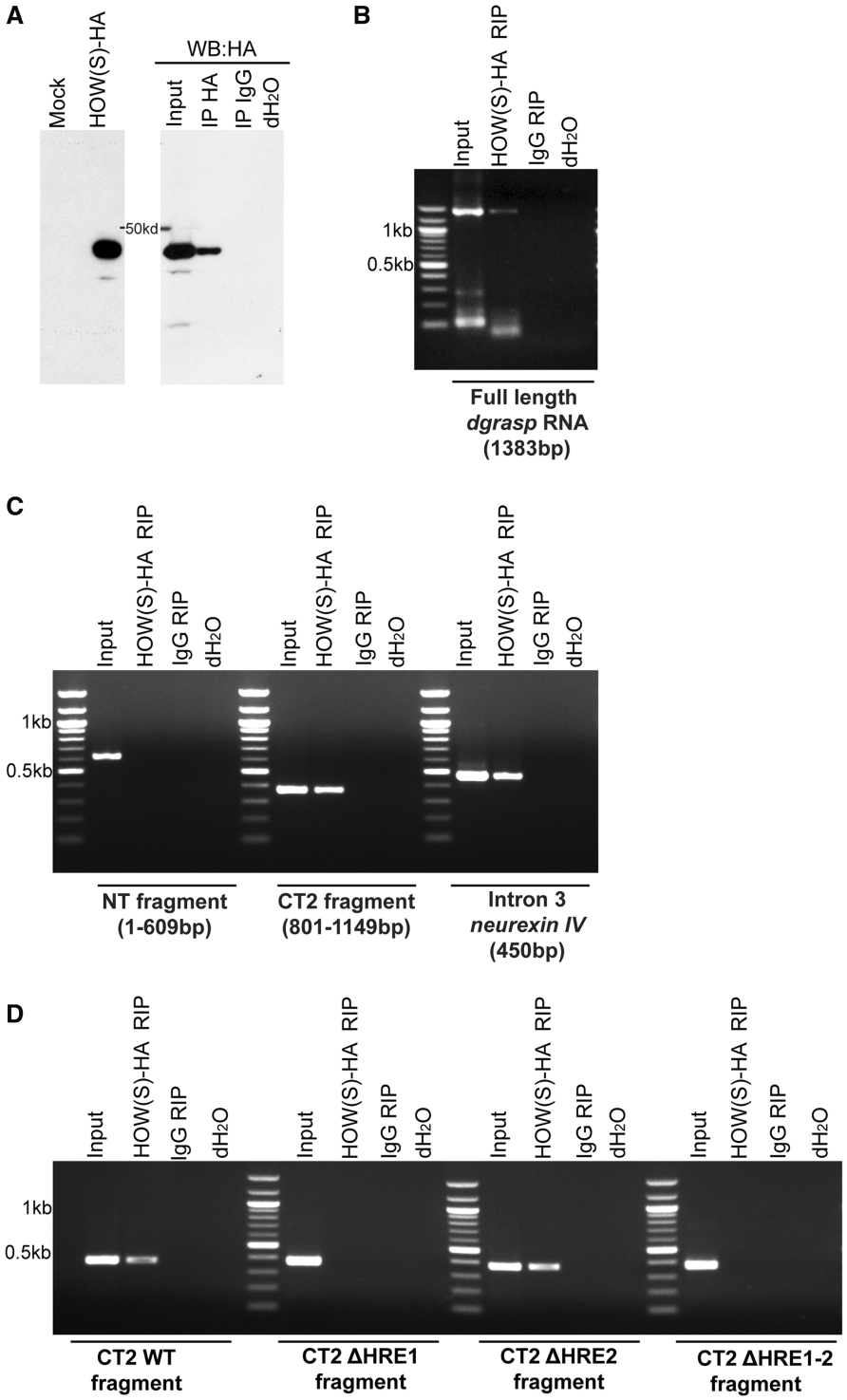

Figure 4. HOW(S) binds *dgrasp* HRE1. (**A**) Western blot detection of *in vitro*-translated HOW(S)-HA upon its synthesis (left panel) and after immunoprecipitation using an anti-HA (HA IP) or IgG as control (IgG IP) (right panel). (**B–D**) Agarose gel electrophoresis of RT–PCR reactions from *in vitro* RIP assays. *In-vitro* synthesized RNAs—full-length *dgrasp* RNA (B); *dgrasp* NT (C); *dgrasp* CT2 (C); *Neurexin IV* intron 3 (C); CT2 ΔHRE1 (D), CT2 ΔHRE2 (D) and CT2 ΔHRE1-2 fragments (D)—were incubated with *in-vitro* synthesized HOW(S)-HA and immunoprecipitated using an anti-HA antibody [HOW(S)HA RIP] or the IgG (IgG RIP).

As expected, in presence of RNase inhibitors, both RNAs were similarly stable overtime (Figure 6A, lanes a, b, e, f, l and j). However, in absence of RNase inhibitors, *dgrasp*-ΔHRE1 mRNA was degraded more rapidly than that of full-length *dgrasp* (63% when compared with 30% after 180 min incubation; $P < 0.05$ c versus k; $P < 0.001$ d versus l; and $P < 0.001$ k versus l) (Figure 6A, lanes c, d and k, l). This shows that the

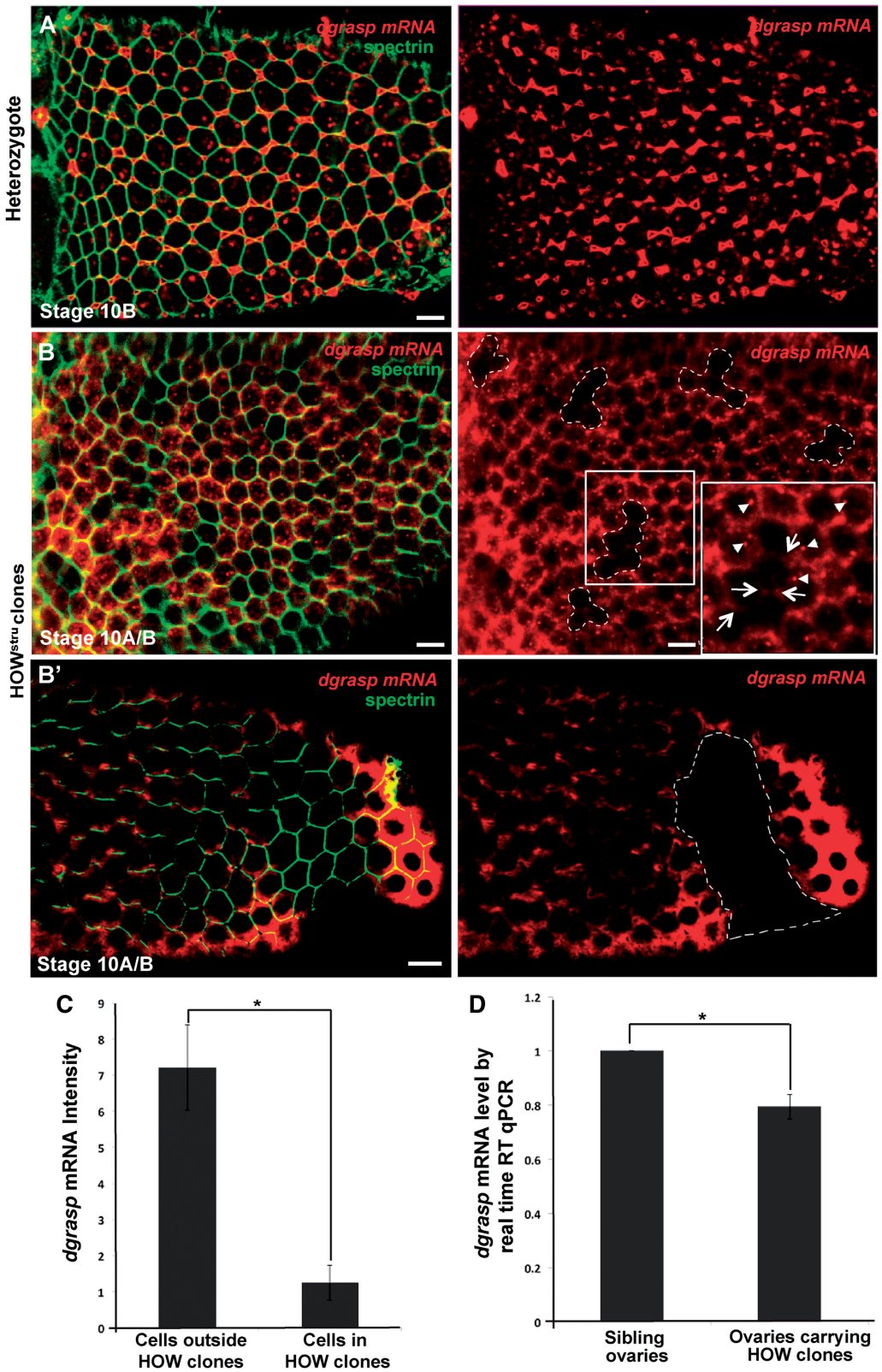

Figure 5. HOW regulates the stability of *dgrasp* mRNA. (**A–B′**) *En face* view of the FISH localization of *dgrasp* mRNA (red) in the follicular epithelium at stage 10B of siblings non-expressing the flippase ($n = 7$ ovaries) (A), and these displaying $HOW^{stru\text{-}3R\text{-}3}$ clones (outlined with dashed lines, $n = 13$ ovaries). The plasma membrane is outlined by immunolabelling with α-spectrin (green). (**C**) Quantification by imageJ of *dgrasp* FISH intensity in the HOW clones and the neighbouring cells. Bars indicate standard error. Fold change of *dgrasp* mRNA expression between control and $HOW^{stru\text{-}3R\text{-}3}$ mutants is significant ($n = 20$, $^*P < 0.001$). (**D**) Real-time RT–qPCR analysis of *dgrasp* mRNA levels in $HOW^{stru\text{-}3R\text{-}3}$ mutant and control stage 10 single oocytes. Bars indicate standard error. The change in *dgrasp* mRNA levels between control and $HOW^{stru\text{-}3R\text{-}3}$ mutants is significant $^*P < 0.001$. Scale bars: 10 μm.

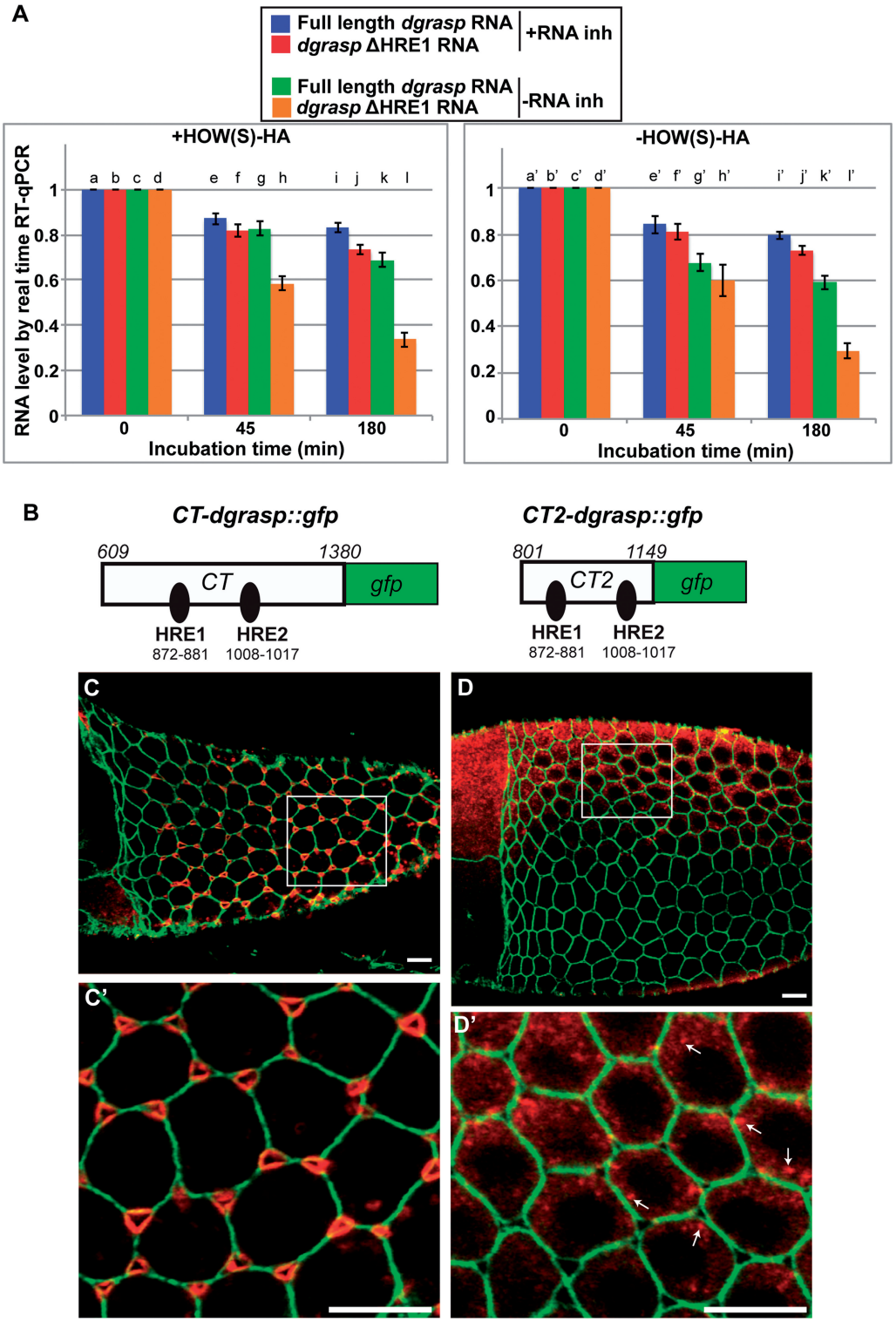

Figure 6. HRE1 is sufficient to mediate *dgrasp* RNA stability but not targeting to the open ZOC. (A) Time course degradation assay of full-length *dgrasp* and *dgrasp-ΔHRE1* RNAs measured by real-time RT–qPCR. Total RNA was isolated at the indicated times (0, 45 and 180 min). The values shown are averages ± SD of three independent experiments performed in duplicate. (**B–C′**) Fluorescent *in situ* hybridization of CT-*dgrasp::gfp* (B) and CT2-*dgrasp::gfp* (C) fragments using anti-sense GFP RNA probe (red) in the follicular epithelium of stage 10B transgenic ovaries overexpressing either of the two *dgrasp* mRNA fragments. Plasma membrane is outlined by immunolabelling with α-spectrin (green). B′ and C′ are insets of C and D, respectively. Note CT2-*dgrasp::gfp* fragment is expressed in the follicular epithelium, but does not localize to the open ZOC. Scale bars: 10 μm.

presence of the HRE1 is necessary for the stability of the *dgrasp* mRNA.

We then assessed the protective role of HOW(S) by performing the same experiment in the absence of exogenous HOW(S)-HA (Figure 6A, lane a′–l′). Both full-length *dgrasp* and *dgrasp*-ΔHRE1 RNAs showed a similar degradation rate in presence of RNase inhibitors, whereas, in the absence of inhibitors, *dgrasp*-ΔHRE1 RNA was again degraded much faster compared with full-length *dgrasp* (compare lane k′ and l′). However, full-length *dgrasp* RNA appeared to be degraded slightly faster at 45 and 180 min in the absence of HOW(S) than in its presence [compare lane g versus g′ ($P < 0.06$) and k versus k′], suggesting a role for HOW(S) in binding HRE1 in *dgrasp* RNA stability. However, this effect as measured in this assay is small probably because Caco-2 cell extracts act as a source of QKI, the mammalian homologue of HOW. Given the highly conserved KH domain, we argue that QKI can bind HRE1, therefore providing stability to the RNA even in the absence of exogenous HOW(S).

Last, an attractive hypothesis is that HOW, in addition to its role in *dgrasp* mRNA protection, is also involved in its targeting to the open ZOC. To test whether HOW binding is sufficient for *dgrasp* mRNA targeting, we examined the localization of the GFP-tagged *dgrasp* CT2 RNA fragment that contained HRE1 (and HRE2) and was shown to bind HOW(S) (Figures 4C, D and 6B), and compared it with the targeting of a fragment encoding the entire C-terminal (CT-*dgrasp*::GFP, Figure 6B). Whereas this latter fragment recapitulates the same dynamics and open ZOC localization as the endogenous *dgrasp* transcript and *dgrasp-GFP* full length (Figure 6C and C′) (13), CT2-*dgrasp*::GFP mRNA forms particles in the cytoplasm (arrows in Figure 6D and D′) but does not efficiently localize to the open ZOCs (Figure 6D and D′). This suggests that HOW binding to HRE1 is not sufficient for *dgrasp* targeting.

In conclusion, we demonstrate that HOW(S) directly binds to one HRE (HRE1) present in the ORF of *dgrasp* mRNA in the cytoplasm of follicle cells at stage 10. There, HOW mediates *dgrasp* mRNA stability by forming RNPs that are then transported to the open ZOC through the interaction with other transacting factors, yet to be identified.

DISCUSSION

Here, we show that in the *Drosophila* follicular epithelium *dgrasp* mRNA directly interacts with HOW, a STAR family RBP, via HRE1 situated in the C-terminus of its ORF. This element is one of two HREs predicted using the RBPDB, and confirmed using the *C. elegans* matrix generated by the Ciosk' laboratory (45). That a *C. elegans* matrix identifies the same motifs corroborates that the sequence making up these sites is conserved throughout evolution and is consistent with the significant sequence conservation of the KH domain of the STAR proteins QKI, HOW and GLD-1.

The functional HRE we characterized, is situated in the *dgrasp* ORF, and not in the 3′UTR as classically reported for QKI/GLD-1 targets. Interestingly, the *C. elegans* homologue of *dgrasp* mRNA (Y42H9AR.1) also displays two predicted HREs in its ORF, suggesting that this feature is conserved. RBPs binding mRNAs in the ORF (including members of the STAR family) are an emerging trend in RNA metabolism with roles in translational repression, transport, as well as stabilization (50). The study of these new targets will open new avenues in the understanding of how RNA metabolism is regulated. In this respect, a crucial step is to determine whether a functional biological bias exists between the bindings of RBPs in the ORF versus the UTRs of a transcript.

HOW, GLD-1 and QKI, have generally been considered to be either translational repressors when bound to the 5′ and 3′UTRs of their targets (45,51) or to modulate alternative splicing when bound to introns (34,52). Here, we show that loss of *HOW* expression in the follicular epithelium results in *dgrasp* degradation, in favour of a role for HOW in stabilization. This is in agreement with an emerging role for the proteins of this family in mRNA stabilization. For instance, zebrafish QKI modulates Hedgehog signalling during muscle-fibre maturation by stabilizing of *Gli2a* mRNA upon binding to the 3′UTR (21). Furthermore, the *C. elegans* GLD-1 is not only a translational repressor but has also been shown to protect its targets during their transport to specific cellular compartments, thus ensuring that they are sufficiently abundant to sustain robust local translation (50). Similarly, during oligodendrocyte differentiation, $p27^{kip}$ mRNA is stabilized upon the binding of QKI7 (53). Interestingly, the QRE in $p27^{kip}$ mRNA also resides in the ORF, as in the case of *dgrasp* mRNA.

As for its orthologues, HOW proteins display multiple isoforms and each one displays a different localization. These isoforms are almost identical in their amino acid sequence, and the only difference resides at the C-terminus, which results in the presence of a NLS in the HOW(L) protein (33). Consistently, our immunohistochemical data show that the longer isoform is restricted to the nucleus, whereas HOW(S) is found in the cytoplasm. A body of evidence from different studies, including this one suggests that although both HOW(L) and HOW(S) proteins are capable of recognizing and binding the same RNA sequence *in vitro,* their RNA substrates seem to differ (30,34,37). In this respect, we show here that the HREs in *Neurexin IV* intron 3 are recognized by both HOW isoforms *in vitro*, but only to HOW(L) *in vivo*. Hence, we propose the different sub-cellular distribution of these HOW isoforms might outline a separation of function and define the substrate specificity.

HOW(S) is also present in punctae near to the basal plasma membrane of the follicle cells at the stage of oogenesis at which *dgrasp* mRNA forms RNPs and is targeted. Accordingly, loss of HOW function leads to the sharp decrease in the amount of *dgrasp* mRNA and the disappearance of the RNPs. One possibility is that HOW is required for *dgrasp* mRNA transport to the open ZOC, perhaps by recruiting motors or adaptors, the absence of which would in turn leads to the mRNA instability. However, although HOW binding to HRE1 is sufficient to form RNPs, it is not sufficient to mediate *dgrasp* localization to the open ZOC. Conversely, we

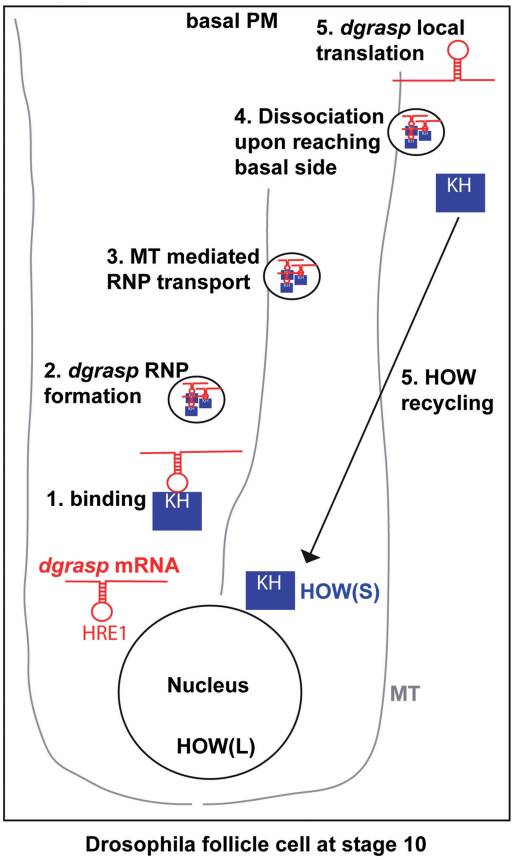

Figure 7. Schematic representation of the role of HOW(S) in *dgrasp* metabolism. Following transcription and nuclear metabolic processes (splicing, 5′-capping and polyadenylation) in stage 10 *Drosophila* follicle cells. The *dgrasp* transcripts are exported into the cytoplasm. There, HOW(S) binds the *dgrasp* mRNA at the HRE1 site via its maxi-KH domain (1) to form together with other factors an RNP that protects *dgrasp* mRNA against degradation (2). *dgrasp* RNPs are then transported near the basal plasma membrane via microtubules (3). Upon reaching destination, *dgrasp* RNPs dissociate (4), HOW(S) is recycled back to the cytoplasm (5) whereas *dgrasp* mRNA is anchored and gets locally translated (5).

show that HOW binding to HRE1 provides stability to *dgrasp* RNA, perhaps by masking it against degradative activities.

We propose the model according to which HOW(S) binding to *dgrasp* HRE1 in the cytoplasm of stage 10 follicle cells regulates the stability of the *dgrasp* transcripts. When HOW is bound to HRE1, it may recruit a RBP complex that is bound either to the 5′ or 3′UTRs of the *dgrasp* mRNA. This complex may in turn prevent the recruitment of the RNA degradation machinery (de-anylation or decapping factors), by hiding signatures that are recognized by RNase complexes. This remains to be investigated.

HOW(S) is then perhaps also involved (although not sufficient) in the transport of *dgrasp* RNPs near the basal membrane in a microtubule-dependent manner (Figure 7). Accordingly, microtubule depolymerization leads RNPs not been targeted to the open ZOC (not shown). Following *dgrasp* localization, HOW(S) would be released to allow *dgrasp* mRNA local translation. The release of HOW interaction is a necessary step as HRE1 resides in the *dgrasp* ORF and would therefore interfere with translation.

HOW loss of function leads to a strong disorganization of the follicular epithelium in line with a role for dGRASP in the delivery of alphaPS1 integrins (13). However, the defects are much stronger because integrins are also a target of HOW, consistent with the up-regulation of *mew* mRNA at the stage 10B (13). It is interesting to note that in this tissue, both the substrate and the machinery are targets of the same RBP. Whether *dgrasp* mRNA metabolism is also regulated by HOW in other tissues and whether HOW is required for the stability of other mRNAs (including those with HRE in the ORF) remains to be investigated.

SUPPLEMENTARY DATA

Supplementary Data are available at NAR Online, including [34].

ACKNOWLEDGEMENTS

The authors thank the members of the Rabouille laboratory for discussion and Adam Grieve, Dominic Grun, Bernardo Blanco-Sanchez and Nerys Williams for critically reading the manuscript; Rafal Ciosk for the use of his GLD-1 matrix prior to publication; Leena Karhinen for generating the transgenic lines carrying the GFP tagged *dgrasp* fragments; Roberto Magliozzi for his help and suggestions on establishing the *in vitro* binding assay. We acknowledge the use of flybase (http://flybase.org/) and the use of Hubrecht Imaging facility (http://www.hubrecht.eu/information/imagingcenter.html) for microscopy.

FUNDING

F.G. and G.G. were supported by ZonMW TOP subsidie [912.080.24 to C.R.]; ISF grant no. [71/12 to T.V.]. Funding for open access charge: ZonMW TOP subsidie [912.080.24], The Netherlands.

Conflict of interest statement. None declared.

REFERENCES

1. Glisovic,T., Bachorik,J., Yong,J. and Dreyfuss,G. (2008) RNA-binding proteins and post-transcriptional gene regulation. *FEBS lett.*, **582**, 1977–1986.
2. Lasko,P. (2003) Gene regulation at the RNA layer: RNA binding proteins in intercellular signaling networks. *Sci. STKE*, **2003**, RE6.
3. Wu,X. and Brewer,G. (2012) The regulation of mRNA stability in mammalian cells: 2.0. *Gene*, **500**, 10–21.
4. Johnstone,O. and Lasko,P. (2001) Translational regulation and RNA localization in Drosophila oocytes and embryos. *Annu. Rev. Genet.*, **35**, 365–406.
5. Tadros,W., Westwood,J.T. and Lipshitz,H.D. (2007) The mother-to-child transition. *Dev. Cell*, **12**, 847–849.
6. Martin,K.C. and Ephrussi,A. (2009) mRNA localization: gene expression in the spatial dimension. *Cell*, **136**, 719–730.

7. Tadros,W. and Lipshitz,H.D. (2005) Setting the stage for development: mRNA translation and stability during oocyte maturation and egg activation in Drosophila. *Dev. Dyn.*, **232**, 593–608.
8. Besse,F. and Ephrussi,A. (2008) Translational control of localized mRNAs: restricting protein synthesis in space and time. *Nat. Rev. Mol. Cell Biol.*, **9**, 971–980.
9. Meignin,C. and Davis,I. (2010) Transmitting the message: intracellular mRNA localization. *Curr. Opi. Cell Biol.*, **22**, 112–119.
10. Vanzo,N., Oprins,A., Xanthakis,D., Ephrussi,A. and Rabouille,C. (2007) Stimulation of endocytosis and actin dynamics by Oskar polarizes the Drosophila oocyte. *Dev. Cell*, **12**, 543–555.
11. Stitzel,M.L. and Seydoux,G. (2007) Regulation of the oocyte-to-zygote transition. *Science*, **316**, 407–408.
12. Zimyanin,V., Lowe,N. and St Johnston,D. (2007) An Oskar-dependent positive feedback loop maintains the polarity of the Drosophila oocyte. *Curr. Biol.*, **17**, 353–359.
13. Schotman,H., Karhinen,L. and Rabouille,C. (2008) dGRASP-mediated noncanonical integrin secretion is required for Drosophila epithelial remodeling. *Dev. Cell*, **14**, 171–182.
14. Schotman,H., Karhinen,L. and Rabouille,C. (2009) Integrins mediate their unconventional, mechanical-stress-induced secretion via RhoA and PINCH in Drosophila. *J. Cell Sci.*, **122**, 2662–2672.
15. Vinke,F., Grieve,A. and Rabouille,C. (2011) The multiple facets of the Golgi reassembly stacking proteins. *Biochem. J.*, **433**, 423–433.
16. Rabouille,C., Malhotra,V. and Nickel,W. (2012) Diversity in unconventional protein secretion. *J. Cell Sci.*, **125**, 5251–5255.
17. Paronetto,M.P., Messina,V., Bianchi,E., Barchi,M., Vogel,G., Moretti,C., Palombi,F., Stefanini,M., Geremia,R., Richard,S. *et al.* (2009) Sam68 regulates translation of target mRNAs in male germ cells, necessary for mouse spermatogenesis. *J. Cell Biol.*, **185**, 235–249.
18. Suzuki,K. and Zagoren,J.C. (1977) Quaking mouse: an ultrastructural study of the peripheral nerves. *J. Neurocytol.*, **6**, 71–84.
19. Ebersole,T., Chen,Q., Justice,M. and Artzt,K. (1996) The quaking gene product necessary in embryogenesis and myelination combines features of RNA binding and signal transduction proteins. *Nat. Genet*, **12**, 260–265.
20. Wu,J., Reed,R., Grabowski,P. and Artzt,K. (2002) Function of quaking in myelination: regulation of alternative splicing. *Proc. Natl Acad. Sci. USA*, **99**, 4233–4238.
21. Lobbardi,R., Lambert,G., Zhao,J., Geisler,R., Kim,H. and Rosa,F. (2011) Fine-tuning of Hh signaling by the RNA-binding protein Quaking to control muscle development. *Development*, **138**, 1783–1794.
22. Jan,E., Motzny,C., Graves,L. and Goodwin,E. (1999) The STAR protein, GLD-1, is a translational regulator of sexual identity in Caenorhabditis elegans. *EMBO J.*, **18**, 258–269.
23. Jeong,J., Verheyden,J. and Kimble,J. (2011) Cyclin E and Cdk2 control GLD-1, the mitosis/meiosis decision, and germline stem cells in Caenorhabditis elegans. *PLoS Genet.*, **7**, e1001348. doi:10.1371/journal.pgen.1001348.
24. Ohno,G., Hagiwara,M. and Kuroyanagi,H. (2008) STAR family RNA-binding protein ASD-2 regulates developmental switching of mutually exclusive alternative splicing in vivo. *Gene Dev.*, **22**, 360–374.
25. Baehrecke,E. (1997) who encodes a KH RNA binding protein that functions in muscle development. *Development*, **124**, 1323–1332.
26. Fyrberg,C., Becker,J., Barthmaier,P., Mahaffey,J. and Fyrberg,E. (1997) A Drosophila muscle-specific gene related to the mouse quaking locus. *Gene*, **197**, 315–323.
27. Lo,P. and Frasch,M. (1997) A novel KH-domain protein mediates cell adhesion processes in Drosophila. *Dev. Biol.*, **190**, 241–256.
28. Zaffran,S., Astier,M., Gratecos,D. and Sémériva,M. (1997) The held out wings (how) Drosophila gene encodes a putative RNA-binding protein involved in the control of muscular and cardiac activity. *Development*, **124**, 2087–2098.
29. Edenfeld,G., Volohonsky,G., Krukkert,K., Naffin,E., Lammel,U., Grimm,A., Engelen,D., Reuveny,A., Volk,T. and Klambt,C. (2006) The splicing factor crooked neck associates with the RNA-binding protein HOW to control glial cell maturation in Drosophila. *Neuron*, **52**, 969–980.
30. Reuveny,A., Elhanany,H. and Volk,T. (2009) Enhanced sensitivity of midline glial cells to apoptosis is achieved by HOW(L)-dependent repression of Diap1. *Mech. Dev.*, **126**, 30–41.
31. Volk,T. (2010) Drosophila star proteins. In: Volk,T. and Artzt,K. (eds), *Post-Transcriptional Regulation by STAR Proteins: Control of RNA Metabolism in Development and Disease*. Springer, USA *Adv. Exp. Med. Biol.*, 693, 93–105.
32. Helit,N.-R., Hila,T.-K., Volohonsky,G. and Volk,T. (2005) Cell divisions in the Drosophila embryonic mesoderm are repressed via posttranscriptional regulation of string/cdc25 by HOW. *Curr. Biol.*, **15**, 295–302.
33. Sette,C. (2010) Post-translational Regulation of STAR Proteins and Effects on Their Biological Functions. In: Volk,T. and Artzt,K. (eds), *Post-Transcriptional Regulation by STAR Proteins: Control of RNA Metabolism in Development and Disease*. Springer, USA. *Adv. Exp. Med. Biol.*, 693, 54–66.
34. Rodrigues,F., Thuma,L. and Klambt,C. (2012) The regulation of glial-specific splicing of Neurexin IV requires HOW and Cdk12 activity. *Development*, **139**, 1765–1776.
35. Cook,K., Kazan,H., Zuberi,K., Morris,Q. and Hughes,T. (2011) RBPDB: a database of RNA-binding specificities. *Nucleic Acids Res.*, **39**, D301–D308.
36. Golic,K. and Lindquist,S. (1989) The FLP recombinase of yeast catalyzes site-specific recombination in the Drosophila genome. *Cell*, **59**, 499–509.
37. Volohonsky,G., Edenfeld,G., Klambt,C. and Volk,T. (2007) Muscle-dependent maturation of tendon cells is induced by post-transcriptional regulation of stripeA. *Development*, **134**, 347–356.
38. Li,J., Ebata,A., Dong,Y., Rizki,G., Iwata,T. and Lee,S. (2008) Caenorhabditis elegans HCF-1 functions in longevity maintenance as a DAF-16 regulator. *PLoS Biol.*, **6**.
39. Livak,K. and Schmittgen,T. (2001) Analysis of relative gene expression data using real-time quantitative PCR and the 2(-Delta Delta C(T)) method. *Methods*, **25**, 402–408.
40. Agy,M., Sherbert,C. and Katze,M. (1996) Development of an in vitro mRNA degradation assay utilizing extracts from HIV-1- and SIV-infected cells. *Virology*, **217**, 158–166.
41. Krikorian,C. and Read,G. (1991) In vitro mRNA degradation system to study the virion host shutoff function of herpes simplex virus. *J. Virol.*, **65**, 112–122.
42. Rio,D., Ares,M., Hannon,G. and Nilsen,T. (2010) Purification of RNA using TRIzol. *Cold Spring Harb. Protoc.*, **2010**, pdb.prot5439. doi: 10.1101/pdb.prot543.
43. Brand,A. and Perrimon,N. (1993) Targeted gene expression as a means of altering cell fates and generating dominant phenotypes. *Development*, **118**, 401–415.
44. Masuda,A., Andersen,H., Doktor,T., Okamoto,T., Ito,M., Andresen,B. and Ohno,K. (2012) CUGBP1 and MBNL1 preferentially bind to 3′ UTRs and facilitate mRNA decay. *Sci. Rep.*, **2**, 209.
45. Wright,J., Gaidatzis,D., Senften,M., Farley,B., Westhof,E., Ryder,S. and Ciosk,R. (2011) A quantitative RNA code for mRNA target selection by the germline fate determinant GLD-1. *EMBO J.*, **30**, 533–545.
46. H,N.-R., Dorevitch,N., Reuveny,A. and Volk,T. (1999) The balance between two isoforms of the Drosophila RNA-binding protein how controls tendon cell differentiation. *Mol. Cell*, **4**, 573–584.
47. H,N.-R., Volohonsky,G., Reuveny,A., R,Z.-B. and Volk,T. (2002) Two isoforms of the Drosophila RNA binding protein, how, act in opposing directions to regulate tendon cell differentiation. *Dev. Cell*, **2**, 183–193.
48. Phelps,C.B. and Brand,A.H. (1998) Ectopic gene expression in Drosophila using GAL4 system. *Methods*, **14**, 367–379.
49. Prout,M., Damania,Z., Soong,J., Fristrom,D. and Fristrom,J. (1997) Autosomal mutations affecting adhesion between wing surfaces in Drosophila melanogaster. *Genetics*, **146**, 275–285.

50. Scheckel,C., Gaidatzis,D., Wright,J. and Ciosk,R. (2012) Genome-wide analysis of GLD-1-mediated mRNA regulation suggests a role in mRNA storage. *PLoS Genet.*, **8**, e1002742.
51. Jungkamp,A.-C., Stoeckius,M., Mecenas,D., Grun,D., Mastrobuoni,G., Kempa,S. and Rajewsky,N. (2011) In vivo and transcriptome-wide identification of RNA binding protein target sites. *Mol. Cell*, **44**, 828–840.
52. Novikov,L., Park,J., Chen,H., Klerman,H., Jalloh,A. and Gamble,M. (2011) QKI-mediated alternative splicing of the histone variant MacroH2A1 regulates cancer cell proliferation. *Mol. Cell. Biol.*, **31**, 4244–4255.
53. Larocque,D., Galarneau,A., Liu,H.-N., Scott,M., Almazan,G. and Richard,S. (2005) Protection of p27(Kip1) mRNA by quaking RNA binding proteins promotes oligodendrocyte differentiation. *Nat. Neurosci.*, **8**, 27–33.